Liu et al. Stem Cell Research & Therapy (2020) 11:220
https://doi.org/10.1186/s13287-020-01676-w

Stem Cell Research & Therapy

RESEARCH Open Access

Exosomes derived from mesenchymal stem cells inhibit neointimal hyperplasia by activating the Erk1/2 signalling pathway in rats

Zhihui Liu[1,2], Chao Wu[2,3], Xinliang Zou[1], Weiming Shen[4], Jiacai Yang[5], Xiaorong Zhang[5], Xiaohong Hu[5], Haidong Wang[3], Yi Liao[3] and Tao Jing[1*]

Abstract

Background: Restenosis is a serious problem in patients who have undergone percutaneous transluminal angioplasty. Endothelial injury resulting from surgery can lead to endothelial dysfunction and neointimal formation by inducing aberrant proliferation and migration of vascular smooth muscle cells. Exosomes secreted by mesenchymal stem cells have been a hot topic in cardioprotective research. However, to date, exosomes derived from mesenchymal stem cells (MSC-Exo) have rarely been reported in association with restenosis after artery injury. The aim of this study was to investigate whether MSC-Exo inhibit neointimal hyperplasia in a rat model of carotid artery balloon-induced injury and, if so, to explore the underlying mechanisms.

Methods: Characterization of MSC-Exo immunophenotypes was performed by electron microscopy, nanoparticle tracking analysis and western blot assays. To investigate whether MSC-Exo inhibited neointimal hyperplasia, rats were intravenously injected with normal saline or MSC-Exo after carotid artery balloon-induced injury. Haematoxylin-eosin staining was performed to examine the intimal and media areas. Evans blue dye staining was performed to examine re-endothelialization. Moreover, immunohistochemistry and immunofluorescence were performed to examine the expression of CD31, vWF and α-SMA. To further investigate the involvement of MSC-Exo-induced re-endothelialization, the underlying mechanisms were studied by cell counting kit-8, cell scratch, immunofluorescence and western blot assays.

Results: Our data showed that MSC-Exo were ingested by endothelial cells and that systemic injection of MSC-Exo suppressed neointimal hyperplasia after artery injury. The Evans blue staining results showed that MSC-Exo could accelerate re-endothelialization compared to the saline group. The immunofluorescence and immunohistochemistry results showed that MSC-Exo upregulated the expression of CD31 and vWF but downregulated the expression of α-SMA. Furthermore, MSC-Exo mechanistically facilitated proliferation and migration by activating the Erk1/2 signalling pathway. The western blot results showed that MSC-Exo upregulated the expression of PCNA, Cyclin D1, Vimentin, MMP2 and MMP9 compared to that in the control group.

(Continued on next page)

* Correspondence: xnkjt@sohu.com
[1]Department of Cardiology, Southwest Hospital, Army Medical University (Third Military Medical University), Chongqing 400038, China
Full list of author information is available at the end of the article

(Continued from previous page)
Interestingly, an Erk1/2 inhibitor reversed the expression of the above proteins.

Conclusion: Our data suggest that MSC-Exo can inhibit neointimal hyperplasia after carotid artery injury by accelerating re-endothelialization, which is accompanied by activation of the Erk1/2 signalling pathway. Importantly, our study provides a novel cell-free approach for the treatment of restenosis diseases after intervention.

Keywords: MSC-Exo, Endothelial cells, Restenosis, Re-endothelialization, Erk1/2 signalling pathway, Neointimal hyperplasia

Introduction

Vascular injury caused by percutaneous transluminal angioplasty (PTA) or stenting results in neointimal hyperplasia (NIH) by inducing abnormal vascular smooth muscle cells (VSMC) proliferation and migration [1]. Currently, drug-eluting stents have markedly decreased restenosis rates, but delayed arterial healing and late stent thrombosis have emerged as major concerns [2]. Therefore, new approaches or tools are needed to prevent restenosis after vascular damage and, in parallel, functional reconstruction of endothelial cells (EC) may be an effective strategy to inhibit the occurrence of NIH.

Mesenchymal stem cells (MSC) are multipotent and capable of being easily isolated from a variety of tissues, such as bone marrow, adipose and cord blood [3]. In addition, it is well known that MSC can secrete proangiogenic and cytoprotective factors through cell-to-cell communication [4]. Based on these attractive properties, MSC are recognized as tissue-repairing cells that may provide safe and effective cardiovascular cell therapies [5]. Moreover, accumulating evidence from in vivo and in vitro studies suggested that some of these reparative effects were mediated by paracrine factors secreted by MSC [6–9]. Recently, the biological factors in conditioned medium, including exosomes and soluble factors, derived from MSC have been extensively studied in different diseases, such as liver injury [10], glioma [11] and cardiovascular disease [12]. Compared with MSC, exosomes derived from mesenchymal stem cells (MSC-Exo) are more stable and storable, have no risk of aneuploidy, a lower possibility of immune rejection following allogeneic administration, and may provide alternative therapies for a variety of diseases [13].

Exosomes, also known as extracellular vesicles, are typically between 30 and 150 nm in diameter and contain a variety of RNAs, proteins and lipids [14]. Exosomes are secreted by a range of cell types, including MSC, and are transported between cells to regulate intercellular connections under certain conditions [15, 16]. Currently, exosomes are easy to obtain by ultracentrifugation or using purification kits, and they have also been extensively studied in cardiovascular diseases. For example, Li et al. [17] found that exosomes derived from cardiac progenitor cells could promote H9C2 cell growth and survival through the activation of the Akt/mTOR signalling pathway. Similarly, a study into the role of exosomes in the progression of acute myocardial infarction employed exosomes derived from mouse embryonic stem cells and revealed that immediate intramyocardial injection could significantly improve endogenous repair and preserve cardiac function in a mouse infarction model [18]. In another study, Kong et al. [19] revealed that exosomes derived from endothelial progenitor cells could inhibit NIH after carotid artery injury in rats. Thus, exosomes may have the same crucial role as cells in the treatment of diseases. However, to date, MSC-Exo have rarely been studied in neointimal formation following artery damage. Here we investigated the roles of MSC-Exo in the formation of NIH and re-endothelialization after rat carotid artery injury.

Rapid re-endothelialization after vascular damage is significant in restoring normal vascular function, reducing vascular inflammation and preventing adverse remodelling and neointimal formation [20]. Therefore, the present study first explored the underlying molecular mechanisms by which MSC-Exo accelerate the proliferation and migration of EC in vitro. Subsequently, we established a model of rat carotid artery balloon-induced injury to assess the effects of MSC-Exo on neointimal formation in vivo. Taken together, our results demonstrated a novel mechanism by which MSC-Exo can inhibit NIH following rat carotid artery balloon-induced injury, which might be a promising approach or tool and provide potential treatment strategies for cardiovascular protection after intervention.

Materials and methods

Cell culture

Briefly, 4-week-old SD rats (Animal Research Center of the Third Army Medical University, Chongqing, China) were sacrificed by cervical dislocation, followed by aseptic collection of the tibia and femur. The medullary cavity was rinsed using mesenchymal stem cell medium (MSCM) to collect bone marrow cells. Bone marrow cells were cultured in MSCM containing 5% exosome-depleted foetal bovine serum (FBS), 1% mesenchymal stem cell growth supplement and a 1% penicillin/streptomycin (P/S) solution (7501, Sciencell, USA) at 37 °C with 5% CO_2. Then, flow cytometry analysis was performed to select for the MSC that were characterized by positive expression of CD29 (FITC-labelled) and

CD90 (PE-labelled) and negative expression of CD11b (eFluor® 450-labelled). EC derived from rat carotid artery were purchased from the Meixuan Company (Shanghai, China) and cultured in 1640 medium (SH30809, Hyclone, USA) supported with 10% exosome-depleted FBS (SV30087, Hyclone, USA) and 1% P/S solution at 37 °C with 5% CO_2.

Isolation and characterization of mesenchymal stem cell-derived exosomes

After 48 h of culture, the MSC culture medium was harvested and centrifuged at 300*g* for 10 min and 2000*g* for 15 min to remove residual cell debris. The supernatants were subsequently filtered using a 0.22-μm filter membrane to remove larger particles. Exosomes were isolated from the culture medium using the Exo Quick-TC Kit (EXOTC50A-1, System Biosciences, USA) according to the manufacturer's instructions. The pelleted exosomes were resuspended in 200 μL of phosphate buffered saline solution (PBS) and quantified by BCA protein assay kit (R33200, Thermo Fisher, USA). Exosomes were then assessed by transmission electron microscopy (TEM) and nanoparticle tracking analysis (NTA), as per previously described protocols [21, 22]. Exosomes were further verified by western blot analysis of exosome-associated markers including CD81, CD63, HSP70, Calnexin and TSG101.

Internalization of PKH67-labelled exosomes in EC

Purified exosomes were labelled with 2 μmol/L of the fluorescent dye PKH67 (MINI67, Sigma, Germany) by incubation for 5 min at room temperature. Ultracentrifugation was performed to remove any remaining free dye at 120,000*g* for 70 min, followed by two washes with PBS and ultracentrifugation. To analyse the ingestion of exosomes by EC, EC were incubated with PKH67-labelled exosomes for 6 h and then stained with Hoechst 33342 (C1025, Beyotime, China). The internalization of PKH67-labelled exosomes by EC was visualized using a fluorescence microscope (IX73, Olympus).

Cell growth assay

Cell proliferation was assessed using cell counting kit-8 (CCK8) reagent (NQ646, Dojindo, Japan). Briefly, EC were seeded at 5×10^3 cells/well into a 96-well plate. EC were then treated with culture medium derived from mesenchymal stem cells (MSC-CM), culture medium derived from endothelial cells (EC-CM), MSC-Exo, exosome-depleted mesenchymal stem cells culture medium (CM-Exo-free) MSC-Exo + DMSO (SHBH9944, Sigma, Germany), MSC-Exo + Erk1/2 inhibitor (10 μM) [23–25] (SCH772984, Selleck, USA) or PBS and incubated for 24 h, 48 h and 72 h according to previous studies. Ten micrograms/millilitre of MSC-Exo was specifically determined to treat the cells. Then, 10 μL of CCK8 solution was added into each well and incubated in dark for 2 h. The absorbance at 450 nm was detected using Microplate Reader.

Cell migration

EC were seeded at 4×10^5 cells/well into a 24-well plate and cultured for 24 h to reach a fusion rate of 80%. The cells were then scratched with a 200-μL sterile pipette tip. The culture medium was immediately removed and replaced with 1640 medium supplied with MSC-Exo, MSC-Exo + DMSO, MSC-Exo + Erk1/2 inhibitor or PBS. Ten micrograms/millilitre of MSC-Exo was specifically determined to treat the cells. To exclude the effects of proliferation, cells were pretreated with 1640 medium containing 10 μg/μL mitomycin. Subsequently, the wound was monitored under a phase-contrast microscope (Olympus, IX51, Japan), and the percentage of cell closure was calculated by measurements of the scratch width using Image-Pro Plus software.

Immunofluorescence

The indicated cells were fixed, permeabilized, blocked and incubated overnight with primary anti-Ki67 antibody (1:200, Abcam, UK) at 4 °C. Subsequently, the cells were incubated with secondary antibodies (1:100, ZSGB, China) for 1 h and stained with 1× Hoechst 33324 for 5 min at room temperature. The cell slides were mounted with anti-fluorescence quencher (P0126, Beyotime, China) and observed under a fluorescence microscope. For paraffin sections, they were deparaffinized, blocked and then incubated with primary anti-CD31 (1:200, R&D) and anti-von Willebrand factor (1:200, vWF, Abcam) antibodies at 4 °C overnight. Then, the sections were incubated with secondary antibodies (1:100, ZSGB, China) and stained with 1× Hoechst 33324 at room temperature. Subsequently, the sections were observed under a fluorescence microscope.

Western blot

EC and exosomes were lysed with ice cold 1× RIPA lysis buffer supplemented with a protease/phosphatase inhibitor cocktail (KGP2100, Keygen, China) and quantified using a BCA kit. A total of 50 μg of protein for each sample was resolved by standard SDS-PAGE electrophoresis and transferred to a PVDF membrane. After blocking with 1× TBS-T containing 5% non-fat milk, the PVDF membrane was incubated overnight at 4 °C with the following primary antibodies: anti-CD81 (1:1000, NOVUS, USA), anti-CD63 (1:1000, Abcam, UK), anti-TSG101 (1:1000, Abcam, UK), anti-HSP70 (1:1000, R&D, USA), anti-Calnexin (1:1000, Abcam, UK), anti-MMP2 (1:1000, R&D, USA), anti-MMP9 (1:1000, NOVUS, USA), anti-Vimentin (1:1000, Abcam, UK), anti-PCNA (1:1000, CST, USA), anti-CyclinD1 (1:1000, CST, USA), anti-Erk1/2 (1:1000, R&D, USA) and anti-P-

Erk1/2 (1:1000, R&D, USA). Then, the PVDF membrane was incubated with a corresponding horseradish peroxidase-conjugated secondary antibody (ZSGB, Beijing, China) at room temperature for 1 h and detected in chemiluminescent solution (32106, Thermo Fisher, USA).

Animal experiments

Old male rats weighing 300 to 400 g were anaesthetized with an intraperitoneal injection of 5% chloral hydrate (100 mg/kg). The hair on the ventral aspect of the neck region was shaved, and the area was swabbed with 75% ethyl alcohol to expose the right common carotid artery (CCA). After blunt dissection alongside the right CCA toward the carotid artery bifurcation, the right internal carotid artery (ICA) was separated and looped proximally and distally with 8-0 silk suture for temporary blood flow cessation. The CCA and external carotid artery (ECA) were temporarily occluded with artery clips. Subsequently, the ICA underwent transverse arteriotomy, and a 1.5-F balloon catheter was inserted through the ICA to the CCA. The balloon was inflated to 10.0 atm and was then slowly withdrawn by rotation. After removal of the catheter, the ICA was ligated near the bifurcation, and the artery clips in the ECA and CCA were removed. The skin was closed, and the rats were divided into sham operation, normal saline and MSC-Exo groups ($n = 6$/group). In the MSC-Exo group, 1 mL of 100 μg/mL exosomes were intravenously injected every 3 days, and the normal saline group received the same volume of normal saline.

Microscopy of rat carotid artery re-endothelialization

On weeks 2 and 4, the rats were anaesthetized with 5% chloral hydrate and intravenously injected with 2% Evans blue ($n = 6$/group). After 10 min, the rats were euthanized by an overdose of chloral hydrate. The right CCA was harvested and washed with PBS to remove residual blood. The area of nonendothelialization was marked with blue, while the area of re-endothelialization was marked with white. The white area to total area ratio was calculated as an indicator of re-endothelialization. The images were observed and collected using a light microscope (Olympus).

Histochemistry and immunohistochemistry

All three groups of rats were sacrificed on weeks 2 and 4 after the establishment of the carotid artery balloon-induced injury model. The right CCA was harvested and fixed in 4% paraformaldehyde. Then, the CCA samples were dehydrated and embedded in paraffin. The samples were sectioned into 8-μm-thick pieces, followed by staining with haematoxylin and eosin (H&E). The intimal to medial area ratio (I/M) was measured using the Image-Pro Plus software program (Media Cybernetics, Rockville, MD). For immunohistochemistry, the sections were deparaffinized, blocked and then incubated with anti-CD31 (1:200), anti-vWF (1:200) and anti-α-smooth muscle actin (1:200, α-SMA, CST) primary antibodies at 4 °C overnight. The CD31- and vWF-positive areas were calculated according the integrated optical density (IOD) of the yellow-brown stained area using Image-Pro Plus software.

Statistical analysis

Statistical analyses were performed using SPSS.23 software. All data from 3 independent experiments are presented as the means ± SD. The Student t test was performed to compare 2 groups; comparisons among ≥ 3 groups were evaluated via 1–way ANOVA followed by the Bonferroni multiple comparison test. $P < 0.05$ was considered statistically significant.

Results

The identification of MSC

The morphology of MSC was observed under a light microscope. Compared to that in the first generation, the morphology of the third generation MSC became spindle-shaped (Fig. 1a). MSC were cultured to the third generation, and the surface antigens CD11b, CD90 and CD29 on the MSC were detected by flow cytometry. The results showed that 0.17% of cells expressed the negative antigen CD11b, while the positive antigens CD29 and CD90 were expressed by 99.6% and 99.8% of cells, respectively, suggesting a high purity among the cultured MSC in our study (Fig. 1b).

Characterization of mesenchymal stem cell-derived exosomes

Transmission electron microscopy revealed that the isolated exosomes were round-shaped membrane vesicles (Fig. 2a). Particle size analysis showed that size of the exosome particles ranged from 30 to 150 nm (Fig. 2b). To further determine the properties of the exosomes, we measured the expression of exosome-associated protein markers by western blot. Our data showed that MSC and exosome particles expressed the specific proteins CD81, CD63, TSG101 and HSP70, while calnexin was only expressed in MSC (Fig. 2c). In addition, we observed that PKH67-labelled MSC-Exo were effectively internalized by EC and concentrated in the cytoplasmic region (Fig. 2d). These data indicated that the extracted exosomes are consistent with published standards and could be used in subsequent experiments.

MSC-Exo promote the proliferation and migration of endothelial cells

To investigate whether exosomes have an effect on EC, we first measured the cell viability of EC that were treated with the MSC-CM, EC-CM, MSC-Exo and CM-

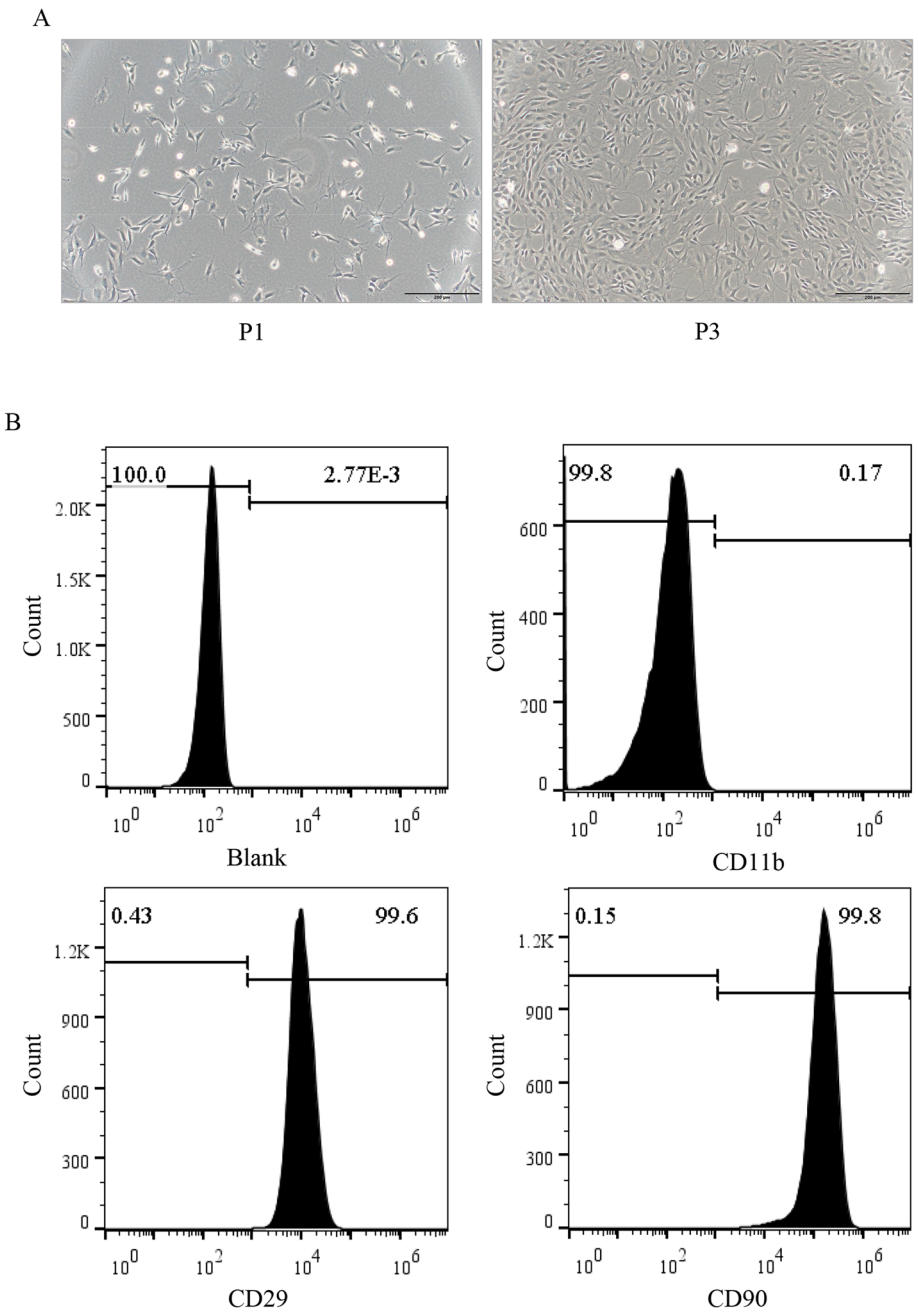

Fig. 1 Characterization of MSC derived from rat bone marrow (RBM). **a** The morphology of the RBM-derived MSC from passage 1 (P1) and 3 (P3) (magnifications, × 100; scale, 50 μm). **b** Flow cytometry results showed that RBM-derived MSC were CD29- and CD90-positive, but CD11b-negative. All figures represent the average of three sets of independent experiments

Exo-free, with untreated EC serving as a control. Our data showed that MSC culture medium, as well as the exosomes extracted from MSC culture medium could significantly promote the growth of EC, while EC culture medium and exosome-deleted MSC culture medium had no effect on EC growth (Fig. 3a, b). Western blot analysis also demonstrated that, compared to the control EC group, the MSC-Exo-treated EC had upregulated expression of PCNA and CyclinD1, which are well-known cell cycle promoting markers (Fig. 3c). Moreover, immunofluorescence further showed that MSC-Exo significantly increased the number of Ki67 positive cells compared to the control EC group, with a percent increase from 68.66% to 90.33% (Fig. 3d, e). These results indicated that the MSC-Exo could promote the proliferation of EC. Further, we investigated whether MSC-Exo

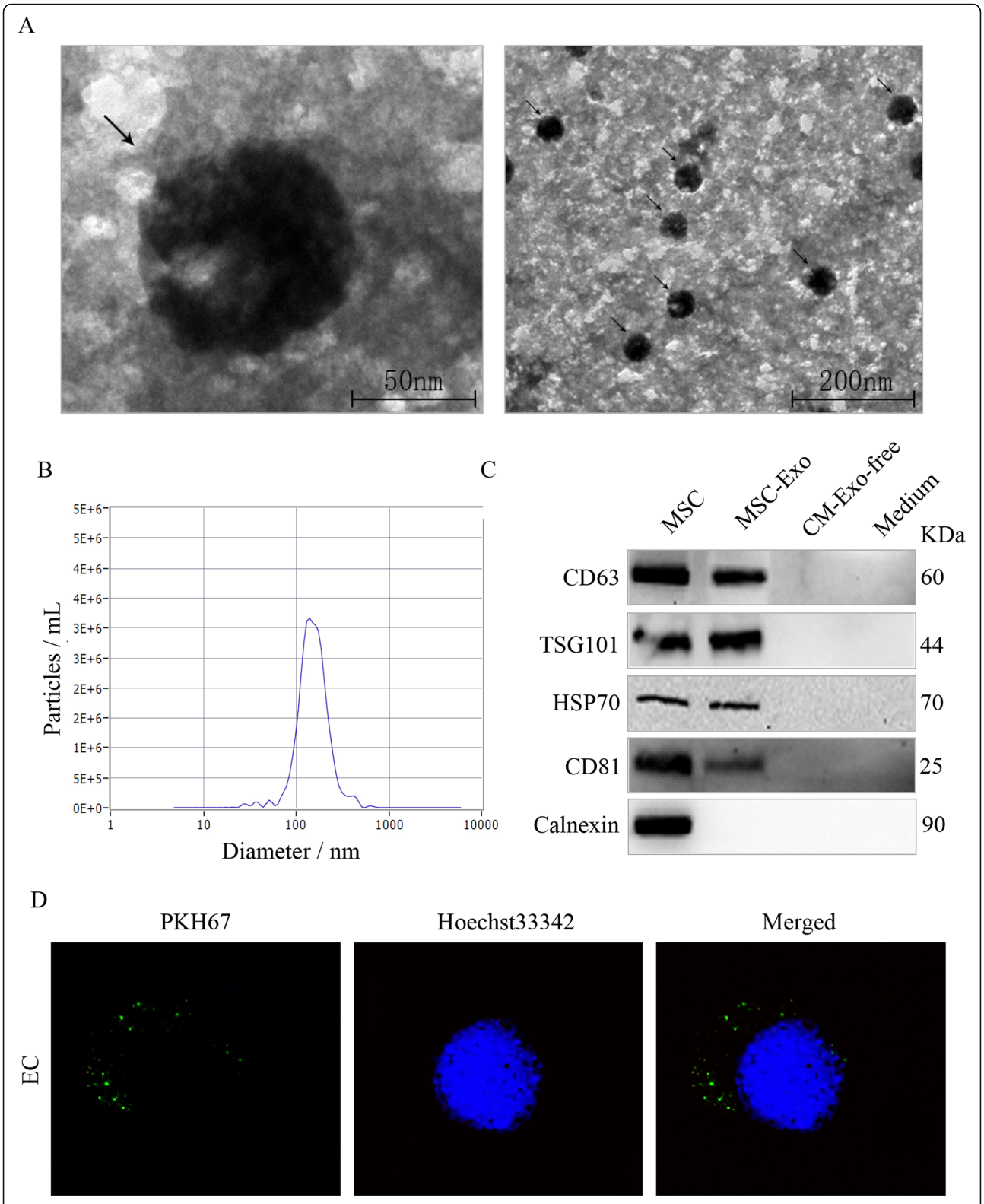

Fig. 2 Characterization of MSC-Exo. **a** Transmission electron microscopy image of exosomes. The black arrows indicate exosomes. **b** Nanoparticle tracking analysis of the size of MSC-Exo. **c** Western blot analysis of the expression of characteristic exosomal proteins (CD63, TSG101, HSP70, CD81). **d** The internalization of PKH67-labelled MSC-Exo (green) by EC after 6 h of incubation (magnifications, × 1000). All figures represent the average of three sets of independent experiments

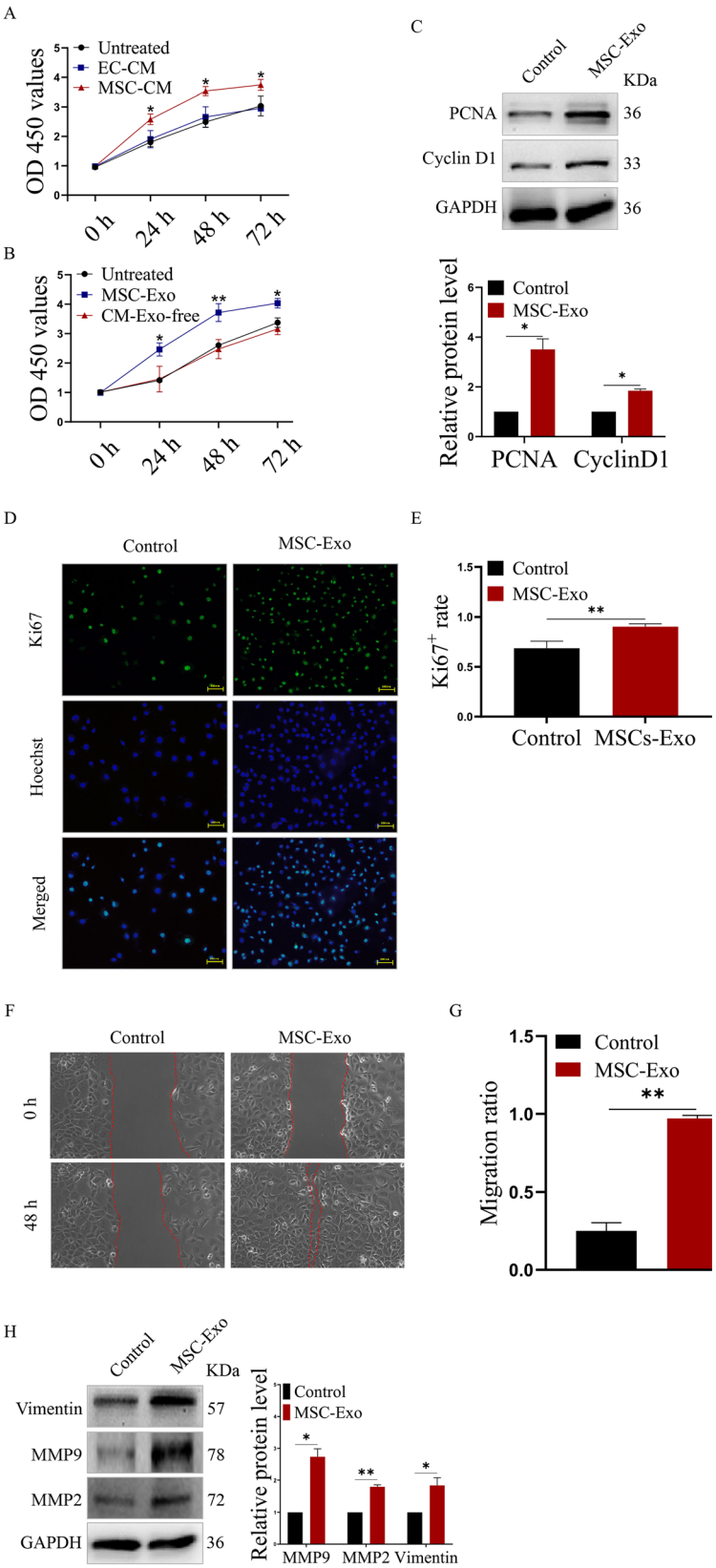

Fig. 3 (See legend on next page.)

(See figure on previous page.)
Fig. 3 MSC-Exo accelerated the proliferation and migration of EC. **a** Cell growth analysis of MSC-CM-treated EC; EC-CM-treated EC served as the negative control group. **b** Cell growth analysis of MSC-Exo-treated EC; CM-Exo-free-treated EC served as the negative control group. **c** Western blot analysis of the expression of induced cell cycle-related proteins. **d** Immunofluorescence analysis of the number of Ki67-positive EC (green) after MSC-Exo treatment (magnifications, × 400; scale, 200 μm). **e** Quantitative analysis of the proportion of Ki67-positive EC. **f** Cell scratch experiment analysis of the migration of EC treated with MSC-Exo. **g** Quantitative analysis of the migration ratio of the indicated EC. **h** Western blot analysis of the expression of induced cell migration-related proteins. $^{*}P < 0.05$ and $^{**}P < 0.01$. All figures represent the average of three sets of independent experiments

could also affect the migration of endothelial cells. Cell scratch experiments were performed in control EC and MSC-Exo-treated EC. Our results showed that MSC-Exo significantly promoted the healing of EC compared to that of the control EC, with a migration ratio increase from approximately 0.25 to 1 (Fig. 3f, g). Western blot analysis also verified that the expression of migration-promoting proteins such as Vimentin, MMP2 and MMP9 were also upregulated (Fig. 3h). These results suggested that MSC-Exo could also promote the migration of EC.

MSC-Exo-induced proliferation and migration of endothelial cells requires Erk1/2 activity

In our study, we found that MSC-Exo could induce the activation of the Erk1/2 signalling pathway in EC by increasing the phosphorylation of the Erk1/2 protein (Fig. 4a). Therefore, we suspected that the Erk1/2 signalling pathway may be involved in MSC-Exo-induced proliferation and migration of EC. To confirm our hypothesis, a specific Erk1/2 inhibitor, SCH772984 (SCH), which inactivates Erk1/2 by blocking phosphorylation [26], was used to determine the role of Erk1/2 activity in the regulation of MSC-Exo-induced proliferation and migration of EC. Our data indicated that SCH could suspend the MSC-Exo-induced the growth of EC (Fig. 4b) and suppress the MSC-Exo-induced migration of EC by reducing the migration ratio from approximately 1 to 0.3 (Fig. 4c, d). Additionally, immunofluorescence further demonstrated that SCH significantly reduced the percentage of Ki67-positive cells to 61.31% in MSC-Exo-treated EC (Fig. 4e, f). Moreover, western blot results showed that SCH inhibits the MSC-Exo-upregulated phosphorylation of the Erk1/2 protein, as well as the expression of downstream proliferation- and migration-related proteins, such as PCNA, CyclinD1, Vimentin, MMP2 and MMP9 (Fig. 4g). Together, these data suggested that MSC-Exo promoted the proliferation and migration of EC through the Erk1/2 signalling pathway.

The effect of MSC-Exo on NIH after carotid injury in vivo

After balloon injury, the injured right CCA of rats were harvested and the re-endothelialization was assessed by Evans blue staining (Fig. 5a). The re-endothelialization ratio of the MSC-Exo group was significantly higher than that of the saline control group after 2 weeks (34.70 ± 10.75% versus 70.28 ± 12.29%, $n = 6$, $P < 0.05$), while there was no significant difference in the re-endothelialization of the carotid artery after 4 weeks (78.33 ± 7.61% versus 83.70 ± 5.25%, $n = 6$, $P = 0.32$) (Fig. 5b). H&E and Masson staining was used to analyse NIH (Fig. 5c). The intimal/media (I/M) was measured as an index. The I/M in the MSC-Exo group was significantly reduced compared to that in the saline group at 2 weeks (0.48 ± 0.06% versus 0.18 ± 0.16%, $n = 6$, $P < 0.01$) and 4 weeks (1.21 ± 0.21 versus 0.50 ± 0.29, $n = 6$, $P < 0.01$) (Fig. 5d). The neointimal and media areas in the MSC-Exo group were both significantly reduced compared to that in the saline group at 2 weeks and 4 weeks (Fig. 5e, f), as well as the collagen area (Fig. 5g). Next, immunohistochemistry was used to examine the proliferation of EC and VSMC (Fig. 5h) after 4 weeks. Our data showed that the balloon injury increased the number of α-SMA-positive cells in the injured CCA; however, treatment with MSC-Exo could reduce this increase (Fig. 5i). Contrarily, compared to the sham control group, the CD31- and vWF-positive areas were significantly decreased in the saline group, while treatment with MSC-Exo reversed this decrease (Fig. 5j, k). In addition, immunofluorescence was used to examine the expression of CD31 and vWF. Our results showed that the treatment of saline could decrease the fluorescence intensity of CD31 and vWF compared to the sham group, while MSC-Exo significantly increased the fluorescence intensity of CD31 and vWF compared to that in the saline group after 4 weeks (Fig. 5l, m). Taken together, these data indicated that MSC-Exo could inhibit NIH by promoting vascular repair and re-endothelialization after vascular injury.

Discussion

All types of intervention result in some degree of arterial injury, the response to which determines the success of the procedure and the long-term prognosis of the patient. Vascular injury is considered to be the main cause of neointimal hyperplasia initiation and progression [27]. Although current strategies to prevent restenosis are focused on the inhibition of neointimal hyperplasia through drug-eluting stents and vascular brachytherapy, restenosis rates following endovascular intervention remain high [22, 28]. Thus, it is important to understand the molecular mechanisms involved in neointima formation.

A previous study demonstrated that MSC derived from bone marrow could inhibit neointimal hyperplasia

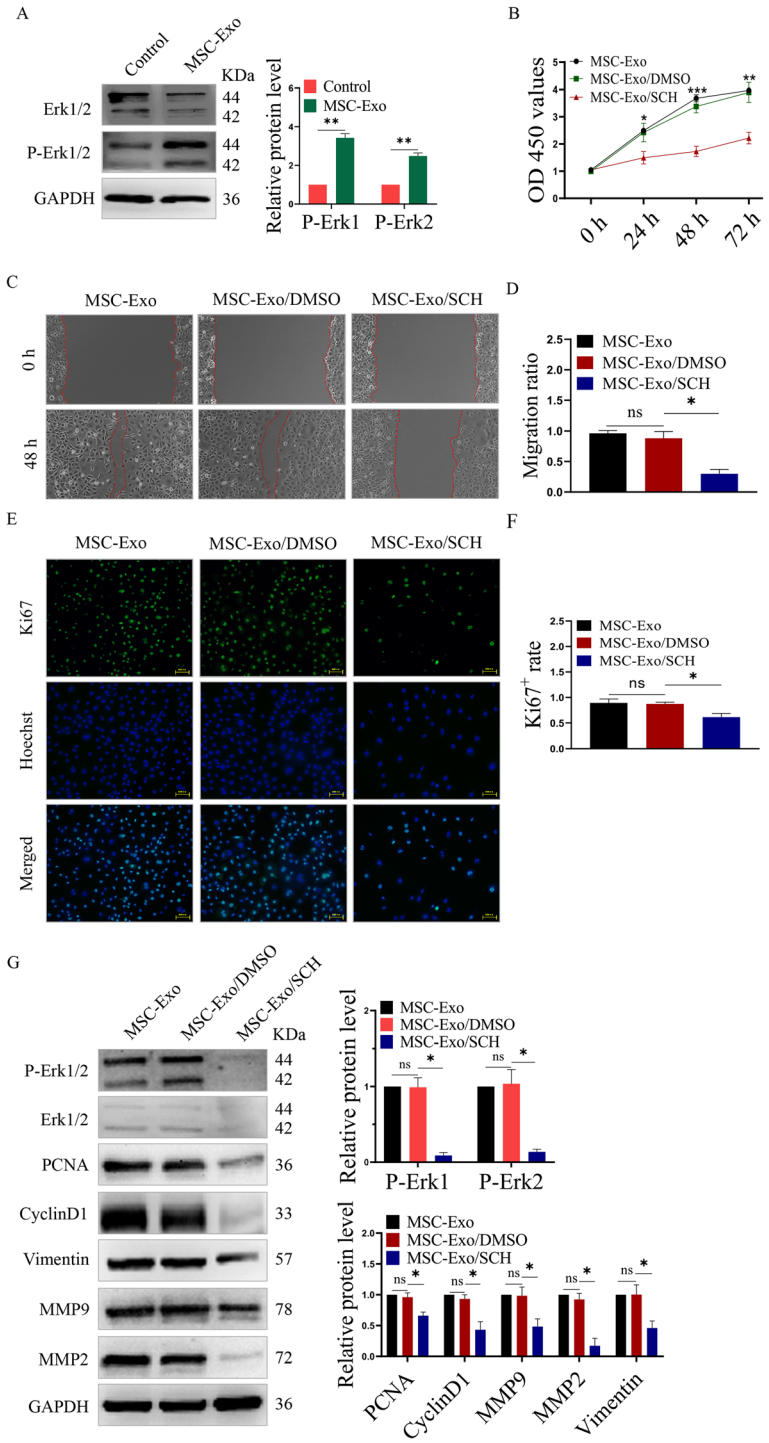

Fig. 4 MSC-Exo activated the Erk1/2 signalling pathway. **a** Western blot analysis of the expression of Erk1/2 and phosphorylated Erk1/2. **b** Cell viability analysis of the growth of EC that were given combined treatment with MSC-Exo and SCH772984. **c** Cell scratch experiment analysis of the migration of EC that were given combined treatment of MSC-Exo and SCH772984. **d** Quantitative analysis of the migration ratio of the indicated EC. **e** Immunofluorescence analysis of the number of Ki67-positive EC (green) after treatment with MSC-Exo and SCH772984 (magnifications, × 400; scale, 200 μm). **f** Quantitative analysis of the proportion of Ki67-positive EC. **g** Western blot analysis of the expression of the indicated proteins. *$P < 0.05$, **$P < 0.01$ and ***$P < 0.001$. All figures represent the average of three sets of independent experiments

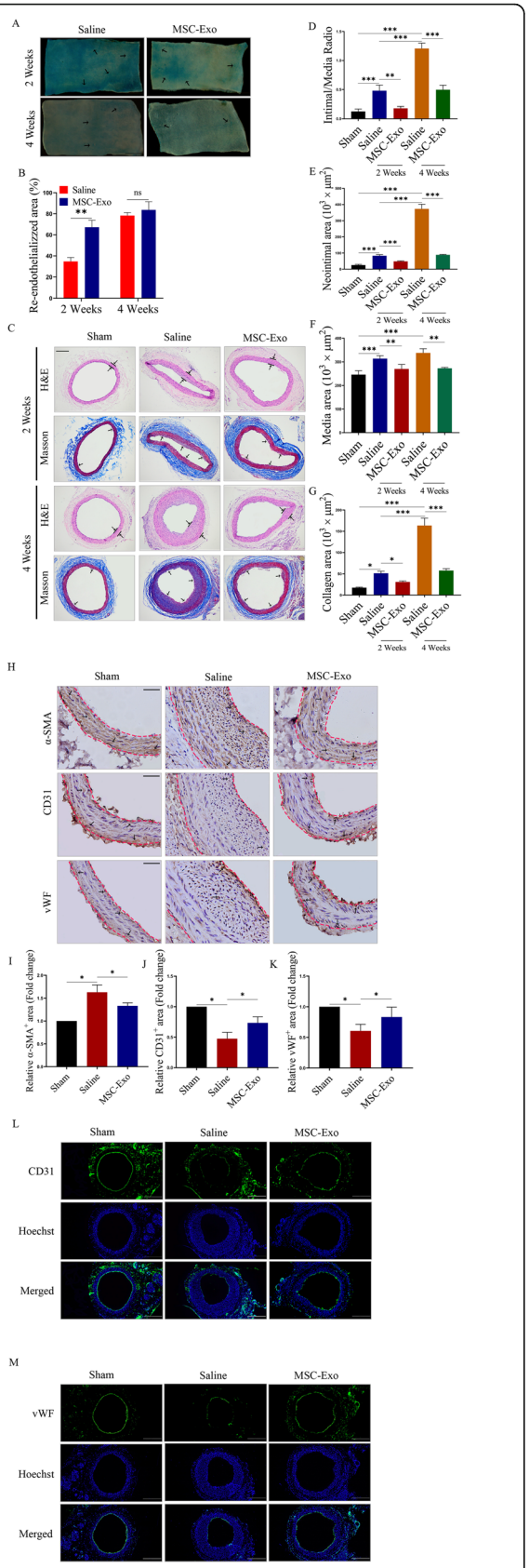

Fig. 5 MSC-Exo inhibited NIH after carotid injury in vivo. **a** Evans blue staining analysis of the re-endothelialization of EC in the injured right CCA of the indicated rats at 2 weeks and 4 weeks ($n = 6$/group) (magnifications, × 40; scale, 200 μm). The black arrows indicate nonendothelialization area. **b** Quantitative analysis of the re-endothelialized areas of the indicated groups. **c** H&E and Masson staining analysis of the formation of neointimal hyperplasia in the indicated rats at 2 weeks and 4 weeks ($n = 6$/group) (magnifications, × 40; scale, 200 μm). The black arrows indicate collagen area. **d** Quantitative analysis of the intimal/media ratio, **e** the neointimal area, **f** the media area and **g** the collagen area of the indicated groups. **h** Immunohistochemical staining analysis of the expression of α-SMA, CD31 and vWF in the indicated rats (magnifications, × 100; scale, 50 μm). The black arrows indicate. Quantitative analysis of the relative **i** α-SMA$^+$, **j** α-CD31$^+$ and **k** vWF$^+$ areas in the indicated rats; data were normalized to the sham group. Representative immunofluorescence images show the expression of **l** CD31 and **m** vWF in the indicated rats (magnifications, × 40; scale, 200 μm). $^*P < 0.05$, $^{**}P < 0.01$ and $^{***}P < 0.001$. All figures represent the average of three sets of independent experiments

after artery injury [29]. They have shown promising effects in experimental models of artery injury and have been used in clinical practice for more than a decade. To date, although advanced stem cell transplantation technology has indeed had beneficial effects on the treatment of cardiovascular disease, the mechanism of this protective effect is generally unclear because of the low efficiency of transdifferentiation into damaged cells after cell transplantation [30]. Interestingly, it was found that MSC improve myocardial function through paracrine effects rather than direct differentiation into cardiomyocytes [12]. Importantly, it has also been reported that MSC have the ability to differentiate into a variety of cell types, such as endothelial cells, smooth muscle cells, myocardium, skeletal muscle and cartilage [31, 32]; however, the beneficial effects of MSC do not depend on their ability to differentiate and replace damaged tissue but are primarily mediated by the release of paracrine factors [33]. Thus, we hypothesized that MSC may affect the NIH of rats through a paracrine network.

In addition to paracrine molecules, a series of secretory membrane-encapsulated vesicles, especially exosomes that participate in a variety of physiological processes, are receiving increasing attention [34]. Exosomes, as a type of extracellular vesicles, originate from the endosomal bodies of cells; endosomes bud inward to form multivesicular bodies (MVBs), which are then fused with the plasma membrane and released into inner vesicles [35]. Generally, transmission electron microscopy, nanoparticle tracking analysis and western blots are used to assess the characterization of these particles. It is through the transfer of their contents, including proteins, lipids and nucleic acid [36], to target cells that exosomes exert functional effects. Increased levels of circulating exosomes have been observed during cardiovascular diseases, including myocardial infarction, and there

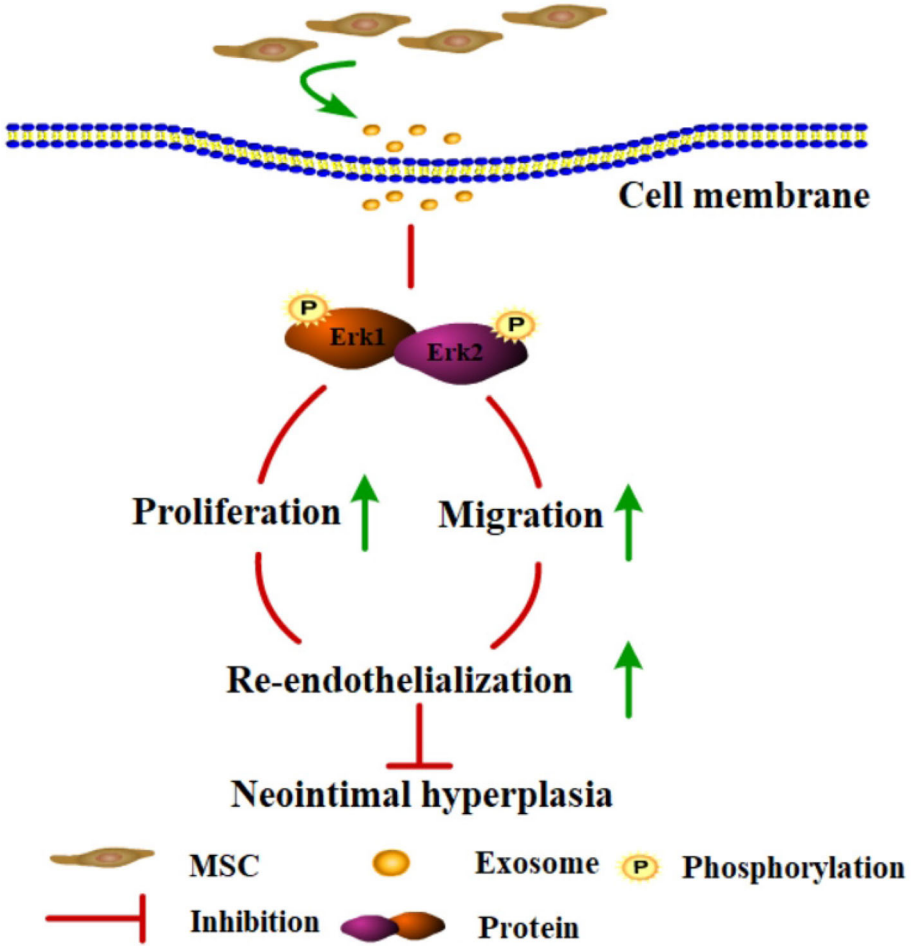

Fig. 6 A working model for how MSC-Exo activation of the Erk1/2 signalling pathway inhibits neointimal hyperplasia via promoting re-endothelialization after vascular injury

is also evidence for a role of exosomes in atherosclerosis, neointima formation and vascular repair and remodelling. However, to date, research into the role of exosomes in disease has relied on exosomes isolated from cultured cells or blood, which may not reflect the in vivo situation. For example, in a rat model of balloon-induced carotid artery injury, exosomes derived from endothelial progenitor cells (EPC) were used to investigate neointima formation and vascular repair, revealing that attenuated vascular repair could enhance re-endothelialization in vivo and endothelial function in vitro [37]. Similarly, a study into the role of exosomes in the progression of atherosclerosis employed exosomes derived from oxidized low-density lipoprotein (oxLDL)-stimulated macrophages and revealed that intravenous administration of oxLDL-treated macrophage cell-derived exosomes into male ApoE-deficient atherosclerosis mice significantly deteriorated atherosclerosis in vivo [38]. In another study, MSC-Exo were shown to exert antiapoptotic and anti-inflammatory effects on intestinal ischaemia-reperfusion-induced lung damage; their effects were accompanied by the downregulation of TLR4 and NF-κB expression, which further protected the lungs against ischeamia-reperfusion-induced acute lung injury [39].

It has been known that the proliferation and migration of smooth muscle cells is exceedingly significant for the initiation and progression of neointimal hyperplasia, but the effects of endothelial cells have also been considered irreplaceable. However, to date, the precise mechanism of endothelial cell influence on the development of neointimal hyperplasia remains obscure. It has been reported that exosomes secreted by a variety of cell types may affect these processes. For example, exosomes derived from endothelial progenitor cells have been shown to limit neointimal hyperplasia and in a study by Kong et al. [19], this was attributed to decreased VSMC proliferation and accelerated re-endothelialization. In another study, Li et al. [40] demonstrated that EC-derived exosomes could repress platelet-derived growth factor (PDGF)-BB-induced phenotypic switching of VSMC and neointimal formation after

carotid injury, while the activation of endothelial CD137 signalling attenuated their effects on VSMC. In addition, there is also evidence showing that exosomes derived from M1 macrophages may exert effects on neointimal hyperplasia via exosomal miRNAs. Exosomes derived from M1 macrophages were shown to aggravate neointimal hyperplasia by delivering miR-222 into VSMC [41]. Therefore, we hypothesized that MSC-Exo may be involved in the process of vascular endothelial cell regeneration and proliferation, which may further inhibit the progression of NIH after carotid injury in rats. Interestingly, our in vitro experiments strongly demonstrated that MSC-Exo could facilitate the proliferation and migration of EC.

Accumulating evidence suggested that MSC-Exo could exert effects via activating/inactivating signalling pathways including the TGF-β1 [42], NF-κB [39, 43] and Wnt [44] signalling pathways. However, to date, the Erk signalling pathway has rarely been studied with MSC-Exo. Furthermore, the Erk signalling pathway is a prototypic mitogen-activated protein kinase (MAPK) signalling cascade that is involved in cell survival, proliferation, migration and differentiation [45, 46]. Several studies also showed that the Erk signalling pathway was closely associated with the growth, survival and migration of cells, whereas these effects were reversed when the signalling pathway was blocked using corresponding inhibitors [47, 48]. Thus, we hypothesized that MSC-Exo could activate/inactivate the Erk signalling pathway during the proliferation and migration of EC. Our experiments further showed that MSC-Exo could promote the proliferation and migration of EC via the Erk1/2 signalling pathway.

Numerous studies have shown that restenosis following endovascular treatment represents an over-healing response to iatrogenic damage to the vessel wall during angioplasty and stenting, which is characterized by the apoptosis of EC and the adhesion and invasion of macrophages, as well as the proliferation and migration of smooth muscle cells [49, 50]. Thus, the accelerated re-endothelialization of the damaged vessels may be significant for the recovery of endothelial function to prevent the formation of a thrombus and excessive neointimal formation. Indeed, our in vivo experiments strongly demonstrated that MSC-Exo could inhibit neointimal formation via accelerated re-endothelialization and the inhibition of VSMC proliferation.

In summary, the present study is the first to demonstrate that MSC-Exo could promote the proliferation and migration of EC, which further accelerated re-endothelialization through the activation of the Erk1/2 signalling pathway, suggesting that MSC-Exo could alleviate the progression of NIH through the Erk1/2 signalling pathway after carotid injury in rats (Fig. 6). However, there are certain limitations to the clinical application of MSC-Exo. Currently, we still face enormous challenges in utilizing exosomes for treatment. First, the minimum effective dose of exosomes needs to be optimized. Second, animal models in addition to the rat should be adopted, including large animal models, such as pigs, rabbits and monkeys. Third, exosome extraction methods need to be further optimized to obtain purer and higher volumes of exosomes. In future studies, we should pay more attention to the biological distribution and bioactivity of exosomes in vivo to determine the optimal treatment window and dosage.

Conclusion

In this study, we have demonstrated that MSC-Exo promoted the proliferation and migration of EC through the Erk1/2 signalling pathway, which accelerated re-endothelialization, thus alleviating the progression of NIH after carotid injury in rats.

Supplementary information

Supplementary information accompanies this paper at https://doi.org/10.1186/s13287-020-01676-w.

Additional file 1.

Abbreviations

CCA: Common carotid artery; CCK8: Cell counting kit-8; CM-Exo-free: Exosome-depleted mesenchymal stem cells culture medium; ECA: External carotid artery; EC: Endothelial cells; EC-CM: Culture medium derived from endothelial cells; EPC: Endothelial progenitor cells; FBS: Foetal bovine serum; H&E: Haematoxylin and eosin; ICA: Internal carotid artery; I/M: Intimal to medial area ratio; IOD: Integrated optical density; MAPK: Mitogen activated protein kinase; MSC: Mesenchymal stem cells; MSC-CM: Culture medium derived from mesenchymal stem cells; MSC-Exo: Exosomes derived from mesenchymal stem cells; MSCM: Mesenchymal stem cell medium; MVBs: Multivesicular bodies; NIH: Neointimal hyperplasia; NTA: Nanoparticle tracking analysis; oxLDL: Oxidized low-density lipoprotein; PBS: Phosphate buffered saline; PDGF: Platelet-derived growth factor; P/S: Penicillin/streptomycin; PTA: Percutaneous transluminal angioplasty; SCH: Erk1/2 inhibitor SCH772984; α-SMA: α-Smooth muscle actin; TEM: Transmission electron microscopy; VSMC: Vascular smooth muscle cells; vWF: von Willebrand factor

Acknowledgements

Thanks for the experimental platform provided by the Institute of Burn Research, South West Hospital AMU (TMMU).

Authors' contributions

Mr. Liu performed the experiments and prepared the first draft of the manuscript. Chao Wu, Xinliang Zou, Weiming Shen, Xinliang Zou, Jiacai Yang, Xiaorong Zhang, Xiaohong Hu and Haidong Wang assisted in the cell culture and data analysis. Dr. Yi Liao and Tao Jing instructed the study and finalized the manuscript. The authors read and approved the final manuscript.

Funding

This work was supported by funds from National Natural Sciences Foundation of China (No. 81370212 to Tao Jing) and the Special Project for Enhancing Science and Technology Innovation Ability (frontier exploration) of Army Military Medical University (Third Military Medical University) (No. 2019XQY13).

Availability of data and materials

The data and materials support that findings could be found.

Ethics approval and consent to participate

In this study, all animal experiments were approved by the Committee on the Use and Care on Animals (The Army Medical University, Chongqing, China) and performed in accordance with institution guidelines.

Consent for publication

Not applicable.

Competing interests

The authors of this article declared that they have no conflict of interests.

Author details

[1]Department of Cardiology, Southwest Hospital, Army Medical University (Third Military Medical University), Chongqing 400038, China. [2]State Key Laboratory of Silkworm Genome Biology, The Institute of Sericulture and Systems Biology, Southwest University, Chongqing, China. [3]Department of Thoracic Surgery, Southwest Hospital, Army Medical University (Third Military Medical University), Chongqing, China. [4]Laboratory of Integrative Medicine, School of Basic Medical Sciences, Shanghai University of Traditional Chinese Medicine, Shanghai, China. [5]The Institute of Burn Research, South-West Hospital, Army Medical University (Third Military Medical University), Chongqing, China.

Received: 6 December 2019 Revised: 17 March 2020
Accepted: 13 April 2020 Published online: 08 June 2020

References

1. Serruys PW, Kutryk MJ, Ong AT. Coronary-artery stents. N Engl J Med. 2006; 354(5):483–95.
2. Finn AV, Nakazawa G, Joner M, Kolodgie FD, Mont EK, Gold HK, Virmani R. Vascular responses to drug eluting stents: importance of delayed healing. Arterioscler Thromb Vasc Biol. 2007;27(7):1500–10.
3. Voswinkel J, Francois S, Simon JM, Benderitter M, Gorin NC, Mohty M, Fouillard L, Chapel A. Use of mesenchymal stem cells (MSC) in chronic inflammatory fistulizing and fibrotic diseases: a comprehensive review. Clin Rev Allergy Immunol. 2013;45(2):180–92.
4. Phinney DG, Prockop DJ. Concise review: mesenchymal stem/multipotent stromal cells: the state of transdifferentiation and modes of tissue repair--current views. Stem Cells. 2007;25(11):2896–902.
5. Karantalis V, Hare JM. Use of mesenchymal stem cells for therapy of cardiac disease. Circ Res. 2015;116(8):1413–30.
6. Hersant B, Sid-Ahmed M, Braud L, Jourdan M, Baba-Amer Y, Meningaud JP, Rodriguez AM. Platelet-rich plasma improves the wound healing potential of mesenchymal stem cells through paracrine and metabolism alterations. Stem Cells Int. 2019;2019:1234263.
7. Jha KA, Pentecost M, Lenin R, Gentry J, Klaic L, Del Mar N, Reiner A, Yang CH, Pfeffer LM, Sohl N, et al. TSG-6 in conditioned media from adipose mesenchymal stem cells protects against visual deficits in mild traumatic brain injury model through neurovascular modulation. Stem Cell Res Ther. 2019;10(1):318.
8. Lu Z, Chang W, Meng S, Xu X, Xie J, Guo F, Yang Y, Qiu H, Liu L. Mesenchymal stem cells induce dendritic cell immune tolerance via paracrine hepatocyte growth factor to alleviate acute lung injury. Stem Cell Res Ther. 2019;10(1):372.
9. Xia X, Chan KF, Wong GTY, Wang P, Liu L, Yeung BPM, Ng EKW, Lau JYW, Chiu PWY. Mesenchymal stem cells promote healing of nonsteroidal anti-inflammatory drug-related peptic ulcer through paracrine actions in pigs. Sci Transl Med. 2019;11(516):7455.
10. Jiang W, Tan Y, Cai M, Zhao T, Mao F, Zhang X, Xu W, Yan Z, Qian H, Yan Y. Human umbilical cord MSC-derived exosomes suppress the development of CCl4-induced liver injury through antioxidant effect. Stem Cells Int. 2018; 2018:6079642.
11. Xu H, Zhao G, Zhang Y, Jiang H, Wang W, Zhao D, Hong J, Yu H, Qi L. Mesenchymal stem cell-derived exosomal microRNA-133b suppresses glioma progression via Wnt/beta-catenin signaling pathway by targeting EZH2. Stem Cell Res Ther. 2019;10(1):381.
12. Suzuki E, Fujita D, Takahashi M, Oba S, Nishimatsu H. Therapeutic effects of mesenchymal stem cell-derived exosomes in cardiovascular disease. Adv Exp Med Biol. 2017;998:179–85.
13. Liao Z, Luo R, Li G, Song Y, Zhan S, Zhao K, Hua W, Zhang Y, Wu X, Yang C. Exosomes from mesenchymal stem cells modulate endoplasmic reticulum stress to protect against nucleus pulposus cell death and ameliorate intervertebral disc degeneration in vivo. Theranostics. 2019;9(14):4084–100.
14. Kishore R, Khan M. More than tiny sacks: stem cell exosomes as cell-free modality for cardiac repair. Circ Res. 2016;118(2):330–43.
15. Hamidi S, Letourneur D, Aid-Launais R, Di Stefano A, Vainchenker W, Norol F, Le Visage C. Fucoidan promotes early step of cardiac differentiation from human embryonic stem cells and long-term maintenance of beating areas. Tissue Eng A. 2014;20(7–8):1285–94.
16. Balaj L, Lessard R, Dai L, Cho YJ, Pomeroy SL, Breakefield XO, Skog J. Tumour microvesicles contain retrotransposon elements and amplified oncogene sequences. Nat Commun. 2011;2:180.
17. Li S, Jiang J, Yang Z, Li Z, Ma X, Li X. Cardiac progenitor cellderived exosomes promote H9C2 cell growth via Akt/mTOR activation. Int J Mol Med. 2018;42(3):1517–25.
18. Khan M, Nickoloff E, Abramova T, Johnson J, Verma SK, Krishnamurthy P, Mackie AR, Vaughan E, Garikipati VN, Benedict C, et al. Embryonic stem cell-derived exosomes promote endogenous repair mechanisms and enhance cardiac function following myocardial infarction. Circ Res. 2015;117(1):52–64.
19. Kong J, Wang F, Zhang J, Cui Y, Pan L, Zhang W, Wen J, Liu P. Exosomes of endothelial progenitor cells inhibit neointima formation after carotid artery injury. J Surg Res. 2018;232:398–407.
20. Kipshidze N, Dangas G, Tsapenko M, Moses J, Leon MB, Kutryk M, Serruys P. Role of the endothelium in modulating neointimal formation: vasculoprotective approaches to attenuate restenosis after percutaneous coronary interventions. J Am Coll Cardiol. 2004;44(4):733–9.
21. Mendez-Barbero N, Gutierrez-Munoz C, Madrigal-Matute J, Minguez P, Egido J, Michel JB, Martin-Ventura JL, Esteban V, Blanco-Colio LM. A major role of TWEAK/Fn14 axis as a therapeutic target for post-angioplasty restenosis. EBioMedicine. 2019;46:274–89.
22. Spadaccio C, Antoniades C, Nenna A, Chung C, Will R, Chello M, Gaudino MFL. Preventing treatment failures in coronary artery disease: what can we learn from the biology of in-stent restenosis, vein graft failure, and internal thoracic arteries? Cardiovasc Res. 2020;116(3):505–19.
23. Lim HS, Kim YJ, Kim BY, Park G, Jeong SJ. The anti-neuroinflammatory activity of tectorigenin pretreatment via downregulated NF-kappaB and ERK/JNK pathways in BV-2 microglial and microglia inactivation in mice with lipopolysaccharide. Front Pharmacol. 2018;9:462.
24. Sale MJ, Minihane E, Monks NR, Gilley R, Richards FM, Schifferli KP, Andersen CL, Davies EJ, Vicente MA, Ozono E, et al. Targeting melanoma's MCL1 bias unleashes the apoptotic potential of BRAF and ERK1/2 pathway inhibitors. Nat Commun. 2019;10(1):5167.
25. Wang ZF, Li J, Ma C, Huang C, Li ZQ. Telmisartan ameliorates Abeta oligomer-induced inflammation via PPARgamma/PTEN pathway in BV2 microglial cells. Biochem Pharmacol. 2020;171:113674.
26. Morris EJ, Jha S, Restaino CR, Dayananth P, Zhu H, Cooper A, Carr D, Deng Y, Jin W, Black S, et al. Discovery of a novel ERK inhibitor with activity in models of acquired resistance to BRAF and MEK inhibitors. Cancer Discov. 2013;3(7):742–50.
27. Ishino M, Shishido T, Suzuki S, Katoh S, Sasaki T, Funayama A, Netsu S, Hasegawa H, Honda S, Takahashi H, et al. Deficiency of long pentraxin PTX3 promoted neointimal hyperplasia after vascular injury. J Atheroscler Thromb. 2015;22(4):372–8.
28. Zotz RJ, Dietz U, Lindemann S, Genth-Zotz S. Coronary restenosis. Herz. 2019;44(1):35–9.
29. Iso Y, Usui S, Toyoda M, Spees JL, Umezawa A, Suzuki H. Bone marrow-derived mesenchymal stem cells inhibit vascular smooth muscle cell proliferation and neointimal hyperplasia after arterial injury in rats. Biochem Biophysics Rep. 2018;16:79–87.
30. Duelen R, Sampaolesi M. Stem cell technology in cardiac regeneration: a pluripotent stem cell promise. EBioMedicine. 2017;16:30–40.
31. Meyer MB, Benkusky NA, Sen B, Rubin J, Pike JW. Epigenetic plasticity drives adipogenic and osteogenic differentiation of marrow-derived mesenchymal stem cells. J Biol Chem. 2016;291(34):17829–47.
32. Diaz D, Munoz-Castaneda R, Alonso JR, Weruaga E. Bone marrow-derived stem cells and strategies for treatment of nervous system disorders: many protocols, and many results. Neuroscientist. 2015;21(6):637–52.
33. Chen YT, Sun CK, Lin YC, Chang LT, Chen YL, Tsai TH, Chung SY, Chua S, Kao YH, Yen CH, et al. Adipose-derived mesenchymal stem cell protects kidneys against ischemia-reperfusion injury through suppressing oxidative stress and inflammatory reaction. J Transl Med. 2011;9:51.
34. Conlan RS, Pisano S, Oliveira MI, Ferrari M, Mendes Pinto I. Exosomes as reconfigurable therapeutic systems. Trends Mol Med. 2017;23(7):636–50.

35. Zhang J, Li S, Li L, Li M, Guo C, Yao J, Mi S. Exosome and exosomal microRNA: trafficking, sorting, and function. Genomics Proteomics Bioinformatics. 2015;13(1):17–24.
36. Colombo M, Moita C, van Niel G, Kowal J, Vigneron J, Benaroch P, Manel N, Moita LF, Thery C, Raposo G. Analysis of ESCRT functions in exosome biogenesis, composition and secretion highlights the heterogeneity of extracellular vesicles. J Cell Sci. 2013;126(Pt 24):5553–65.
37. Li X, Chen C, Wei L, Li Q, Niu X, Xu Y, Wang Y, Zhao J. Exosomes derived from endothelial progenitor cells attenuate vascular repair and accelerate reendothelialization by enhancing endothelial function. Cytotherapy. 2016; 18(2):253–62.
38. Zhang YG, Song Y, Guo XL, Miao RY, Fu YQ, Miao CF, Zhang C. Exosomes derived from oxLDL-stimulated macrophages induce neutrophil extracellular traps to drive atherosclerosis. Cell Cycle. 2019;18(20):2674–84.
39. Liu J, Chen T, Lei P, Tang X, Huang P. Exosomes released by bone marrow mesenchymal stem cells attenuate lung injury induced by intestinal ischemia reperfusion via the TLR4/NF-kappaB pathway. Int J Med Sci. 2019; 16(9):1238–44.
40. Li B, Zang G, Zhong W, Chen R, Zhang Y, Yang P, Yan J. Activation of CD137 signaling promotes neointimal formation by attenuating TET2 and transferrring from endothelial cell-derived exosomes to vascular smooth muscle cells. Biomed Pharmacother. 2020;121:109593.
41. Wang Z, Zhu H, Shi H, Zhao H, Gao R, Weng X, Liu R, Li X, Zou Y, Hu K, et al. Exosomes derived from M1 macrophages aggravate neointimal hyperplasia following carotid artery injuries in mice through miR-222/CDKN1B/CDKN1C pathway. Cell Death Dis. 2019;10(6):422.
42. Lin Y, Zhang F, Lian XF, Peng WQ, Yin CY. Mesenchymal stem cell-derived exosomes improve diabetes mellitus-induced myocardial injury and fibrosis via inhibition of TGF-beta1/Smad2 signaling pathway. Cell Mol Biol. 2019; 65(7):123–6.
43. Shen Y, Xue C, Li X, Ba L, Gu J, Sun Z, Han Q, Zhao RC. Effects of gastric cancer cell-derived exosomes on the immune regulation of mesenchymal stem cells by the NF-kB signaling pathway. Stem Cells Dev. 2019;28(7):464–76.
44. Zuo R, Liu M, Wang Y, Li J, Wang W, Wu J, Sun C, Li B, Wang Z, Lan W, et al. BM-MSC-derived exosomes alleviate radiation-induced bone loss by restoring the function of recipient BM-MSCs and activating Wnt/beta-catenin signaling. Stem Cell Res Ther. 2019;10(1):30.
45. Tanimura S, Takeda K. ERK signalling as a regulator of cell motility. J Biochem. 2017;162(3):145–54.
46. Hutton SR, Otis JM, Kim EM, Lamsal Y, Stuber GD, Snider WD. ERK/MAPK signaling is required for pathway-specific striatal motor functions. J Neurosci. 2017;37(34):8102–15.
47. Perreault S, Larouche V, Tabori U, Hawkin C, Lippe S, Ellezam B, Decarie JC, Theoret Y, Metras ME, Sultan S, et al. A phase 2 study of trametinib for patients with pediatric glioma or plexiform neurofibroma with refractory tumor and activation of the MAPK/ERK pathway: TRAM-01. BMC Cancer. 2019;19(1):1250.
48. Ricard N, Zhang J, Zhuang ZW, Simons M. Isoform-Specific Roles of ERK1 and ERK2 in Arteriogenesis. Cells. 2019;9(1):38.
49. Xu RW, Zhang WJ, Zhang JB, Wen JY, Wang M, Liu HL, Pan L, Yu CA, Lou JN, Liu P. A preliminary study of the therapeutic role of human early fetal aorta-derived endothelial progenitor cells in inhibiting carotid artery neointimal hyperplasia. Chin Med J. 2015;128(24):3357–62.
50. Yan D, Zhang D, Lu L, Qiu H, Wang J. Vascular endothelial growth factor-modified macrophages accelerate reendothelialization and attenuate neointima formation after arterial injury in atherosclerosis-prone mice. J Cell Biochem. 2019;120(6):10652–61.

Publisher's Note